NAVAL POSTGRADUATE SCHOOL
Monterey, California

THESIS

EFFECT OF WATER DEPTH ON THE UNDERWATER WET WELDING OF FERRITIC STEELS USING AUSTENITIC NI-BASED ALLOY ELECTRODES

by

Brian J. Sheakley

September 2000

Thesis Advisor: Alan G. Fox

Approved for public release; distribution is unlimited.

DTIC QUALITY INSPECTED 4

20001120 161

REPORT DOCUMENTATION PAGE

Public reporting burden for this collection of information is estimated to average 1 hour per response, including the time for reviewing instruction, searching existing data sources, gathering and maintaining the data needed, and completing and reviewing the collection of information. Send comments regarding this burden estimate or any other aspect of this collection of information, including suggestions for reducing this burden, to Washington Headquarters Services, Directorate for Information Operations and Reports, 1215 Jefferson Davis Highway, Suite 1204, Arlington, VA 22202-4302, and to the Office of Management and Budget, Paperwork Reduction Project (0704-0188) Washington DC 20503.

1. AGENCY USE ONLY *(Leave blank)*	2. REPORT DATE September 2000	3.REPORT TYPE AND DATES COVERED Master's Thesis
4. TITLE AND SUBTITLE Effect of Water Depth on the Underwater Wet Welding of Ferritic Steels Using Austenitic Ni-based Alloy Electrodes		5. FUNDING NUMBERS
6. AUTHOR(S) Sheakley, Brian J.		
7. PERFORMING ORGANIZATION NAME(S) AND ADDRESS(ES) Naval Postgraduate School Monterey CA 93943-5000		8. PERFORMING ORGANIZATION REPORT NUMBER
9. SPONSORING/MONITORING AGENCY NAME(S) AND ADDRESS(ES) Naval Sea Systems Command (NAVSEA OOC) 2531 Jefferson Davis Hwy Arlington, VA 22242—5160		10. SPONSORING/MONITORING AGENCY REPORT NUMBER

11. SUPPLEMENTARY NOTES The views expressed in this thesis are those of the author and do not reflect the official policy or position of the Department of Defense or the U.S. Government.

12a. DISTRIBUTION/AVAILABILITY STATEMENT Approved for public release; distribution is unlimited	12b. DISTRIBUTION CODE

13. ABSTRACT *(maximum 200 words)*

Underwater welding using shielded metal arc welding (SMAW) on US Naval Vessels is very attractive because of the ability to effect repairs without costly dry dock expenses. In the past the primary problems with underwater wet weldments on steels utilizing SMAW with ferritic electrodes, were underbead cracking in the heat affected zone (HAZ), slag inclusions, oxide inclusions, and porosity.

To avoid underbead cracking three weld samples were made using an austenitic nickel weld metal with an Oxylance coating at 10 feet of salt water, 25 feet of salt water, and 33 feet of salt water. A final sample was made using austenitic nickel weld metal with a Broco coating at 33 feet of salt water. Because of the ductility of the austenitic nickel weld metal no underbead cracking occurred, however porosity and high inclusion counts were found in all four samples. The average size of the inclusion increased with increasing depth. The Broco sample exhibited far greater porosity than did the Oxylance samples. This work addresses quality of the welds, mechanisms for the formation of the inclusions, and analysis of the difference between the Oxylance and Broco weld rods.

14. SUBJECT TERMS: Underwater wet welding, Non-metallic inclusions, Shielded Metal Arc Welding	15. NUMBER OF PAGES : 56
	16. PRICE CODE

17. SECURITY CLASSIFICATION OF REPORT Unclassified	18. SECURITY CLASSIFICATION OF THIS PAGE Unclassified	19. SECURITY CLASSIFICATION OF ABSTRACT Unclassified	20.LIMITATION OF ABSTRACT UL

NSN 7540-01-280-5500

THIS PAGE INTENTIONALLY LEFT BLANK

EFFECT OF WATER DEPTH ON THE UNDERWATER WET WELDING OF FERRITIC STEELS USING AUSTENITIC NI-BASED ALLOY ELECTRODES

Brian J. Sheakley
Lieutenant, United States Navy
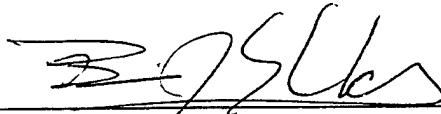B.S. Aerospace Engineering, Illinois Institute of Technology, 1994

Submitted in partial fulfillment of the
requirements for the degree of

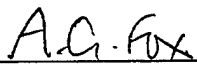## MASTER OF SCIENCE IN MECHANICAL ENGINEERING

from the

NAVAL POSTGRADUATE SCHOOL
September 2000

Author: _____

Brian J. Sheakley

Approved by: _____

Alan G. Fox, Thesis Advisor

_____

Terry R. McNelley, Chairman
Department of Mechanical Engineering

iii

THIS PAGE INTENTIONALLY LEFT BLANK

ABSTRACT

Underwater welding using shielded metal arc welding (SMAW) on US Naval Vessels is very attractive because of the ability to effect repairs without costly dry dock expenses. In the past the primary problems with underwater wet weldments on steels utilizing SMAW with ferritic electrodes, were underbead cracking in the heat affected zone (HAZ), slag inclusions, oxide inclusions, and porosity.

To avoid underbead cracking three weld samples were made using an austenitic nickel weld metal with an Oxylance coating at 10 feet of salt water, 25 feet of salt water, and 33 feet of salt water. A final sample was made using austenitic nickel weld metal with a Broco coating at 33 feet of salt water. Because of the ductility of the austenitic nickel weld metal no underbead cracking occurred, however porosity and high inclusion counts were found in all four samples. The average size of the inclusion increased with increasing depth. The Broco sample exhibited far greater porosity than did the Oxylance samples.

This work addresses quality of the welds, mechanisms for the formation of the inclusions, and analysis of the difference between the Oxylance and Broco weld rods.

THIS PAGE INTENTIONALLY LEFT BLANK

TABLE OF CONTENTS

ACKNOWLEDGMENTS

I would like to sincerely thank Professor Alan G. Fox for his wisdom, guidance, support, and confidence in me throughout the thesis research process. I would also like to thank Professor Sarath K. Menon for his support, guidance, and instruction with the laboratory equipment. Without their assistance I would have been without direction and would have aimlessly struggled through the process.

I would also like to thank my family, who have always had the utmost confidence in me and have tirelessly supported me throughout my career. Thank you from the bottom of my heart.

THIS PAGE INTENTIONALLY LEFT BLANK

I. INTRODUCTION

The study of the U.S. Navy use of underwater wet welding has been ongoing at Naval Postgraduate School since 1997. This process of welding, using the Shielded Metal Arc Welding (SMAW) process, has been analyzed for possible use in ship repair. This type of ship repair process is of particular interest to the U.S. Navy to avoid dry-docking to effect repairs and to extend the period between major overhauls. However, because of rapid cooling rates and the presence of excess hydrogen and oxygen, prevalent in underwater operations, the use of ferric steel weld electrodes for the underwater welding of ferritic steels with a carbon equivalent (CE) greater than 0.38 wt% has often proven difficult because of underbead cracking in the heat affected zone (HAZ).

Based on results from research into the use of ferritic steels for underwater wet welding, it was decided to try an austenitic nickel-based electrode to prevent underbead cracking in steels with higher CE. The current research studies the weld procedure and quality of the weld to determine the feasibility of using this procedure for ship repair.

THIS PAGE INTENTIONALLY LEFT BLANK

II. BACKGROUND

A. UNDERWATER WET WELDING

Underwater wet welding processes are classified by the American Welding Society in [Ref. 1]. These processes are defined by having the welder and associated work in direct contact with the underwater environment. The specifications for underwater wet welding can be found in Specification for Underwater Welding [Ref. 1].

B. UNDERWATER WET SHIELDED METAL ARC WELDING

The process most commonly used for wet weldments is the Shielded Metal Arc Welding (SMAW) process [Ref. 2]. The base metal and the electrode, used in underwater SMAW, must be selected carefully. The electrodes selected must avoid water intrusion into the flux of the electrode as much as possible. The safety gear required to be worn by welder/diver restricts movement, but is required. Due to high current of SMAW, the electrical safety of the welder/diver is a top priority. Typical equipment set up of underwater operations is outlined in the U.S. Navy Underwater Cutting and Welding Manual [Ref. 3]. The equipment set up is shown in Figure 2.1. Underwater SMAW is almost identical to SMAW process performed on the surface. The major differences are the electrodes, which consist of a waterproof coating and specials fluxes to reduce water absorption. Also, a direct current straight polarity (DCSP) is selected for the safety of the welder/diver and welding/safety equipment is remote to the work. Apart from these differences the SMAW process is similar to that shown in Figure 2.2 [Ref. 4].
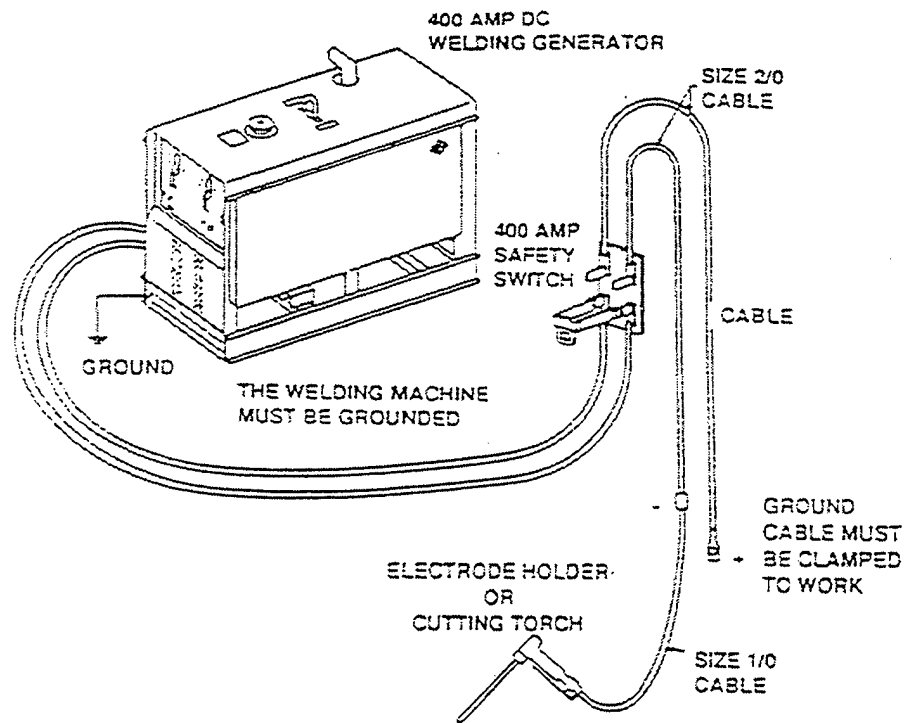
3

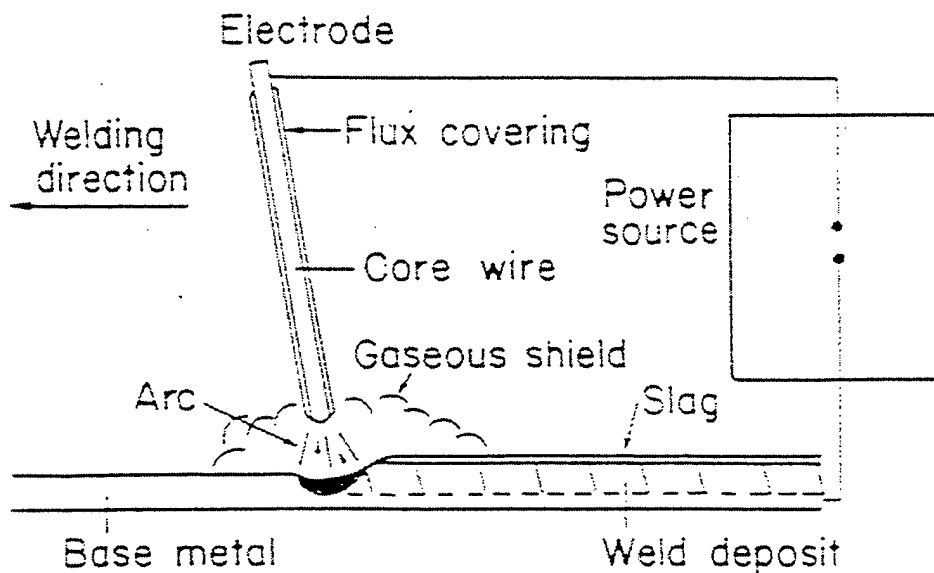Figure 2.1 SMAW set up for underwater operations [Ref. 3]

Figure 2.2 SMAW welding process [Ref. 4]

C. THE HAZ MICROSTRUCTURE OF FERRITIC STEEL IN AN UNDERWATER WET WELDING ENVIRONMENT

1. Rapid Cooling Rate

When operating SMAW in an underwater environment, the welds are subjected to increased cooling rates that have an effect on the microstructure of the heat affected zone (HAZ). This is shown in Table 2.1 from [Ref. 5]. From this table it can be seen that the cooling times at the fusion line during underwater wet welding for a change in temperature from 800°C to 500°C with a water temperature of 2°C or 31°C is approximately two times faster than the cooling rate predicted in air, at a temperature of 20°C calculated by Rosenthal's equation. Microstructure morphologies that are most commonly associated with the rapid cooling rates in underwater operations on ferritic steels are martensite and banite. These microstructures are particularly evident when wet welding stronger steels (carbon equivalent (CE) > 0.4 wt%), where CE is defined as:

$$CE = C + (Mn + Si)/6 + (Ni + Cu)/15 + (Cr + Mo + V)/5. \qquad 2.1$$

Because of the need to obtain a fusion zone that is close to the strength of the base metal, it is difficult to weld stronger ferritic steels with ferritic electrodes without underbead cracking occurring because of limited weld metal ductility. Another major difficulty in underwater wet welding is avoiding hydrogen accumulation in the weld metal and the HAZ. This occurs when the arc formed in the welding process dissociates water into hydrogen and oxygen. As a consequence of the increased hydrogen and the brittle martensitic microstructure, the HAZ is susceptible to underbead cracking as described in [Ref. 6] and [Ref. 7]. This research demonstrated a large amount of underbead cracking in ferritic steels underwater wet welded with ferritic electrodes. Another difficulty with

underwater wet welding operations is that porosity may be encountered during the

solidification of the weld metal especially when welding in the overhead position.

However, in the past this has not proved a problem when using ferritic electrodes [Ref. 6]

and [Ref. 7].

Water Temperature [C]	Position	Weld Speed [ipm]	Power Input [kW]	Plate Thickness [in]	$\Delta t_{800-500}$
Current Model					
2	Fusion Line	6.5	3.9	¾	1.14
31	Fusion Line	6.5	3.9	¾	1.20
Tsai et al. Model					
0	1mm from Fusion Line	9	5.0	1/8	1.85
27	1mm from Fusion Line	9	5.0	1/8	1.90
Rosenthal's Model					
20*	Fusion Line	6.5	3.9	∞	2.38
* Plate Temperature prior to welding.					

Table 2.1 Cooling rates for underwater wet welding [Ref. 5]. Note that the calculations using Rosenthal's model are for a welding operation carried out in air.

2. Material Selection

One effective method for preventing underbead cracking is to attempt to prevent

excessive/hard martensite formation. This method involves controlling the carbon

equivalent (CE) of the base metal and the electrode. The CE of a ferritic steel is

determined by Equation 2.1 and is set at a maximum of 0.4 wt% by [Ref. 1], but even this

can be too high for underwater wet welding of steels in cold water as discussed in [Ref. 6]

and [Ref. 7].

The CE must be compared when selecting the base metal and weld metal. This

can be seen in Figure 2.3, which shows the zones of weldability for various CE base

6

plates. The solid lines in Figure 2.3 relate to welding in air. A CE of approximately 0.38 wt% (0.1 wt% carbon), which is indicated by the dotted line in Figure 2.3, is recommended by [Ref. 6] for wet welds. The dashed line in Figure 2.3 represents a CE of approximately 0.4 wt% (0.1 wt% carbon), discussed earlier. An increase in ductility is found in metals with lower CE. Therefore, to attempt to prevent underbead cracking a base plate with a lower CE can be used or, alternatively, steel base plates with carbon contents of less than 0.1 wt% can be welded, although, as yet, these are not in common use on ships. High strength steels may not be underwater wet weldable even if a weld metal of lower strength is used. This is because undermatched weld metal may still be insufficiently ductile to prevent underbead cracking despite having a lower strength than the base plate. Indeed, even mild steel weld metals may not be ductile enough to prevent underbead cracking when welding steels with CE 0.4 wt% (0.2 wt% carbon) [Ref. 6] and [Ref.7]. These weld metals do however achieve sufficient strength for this particular application.
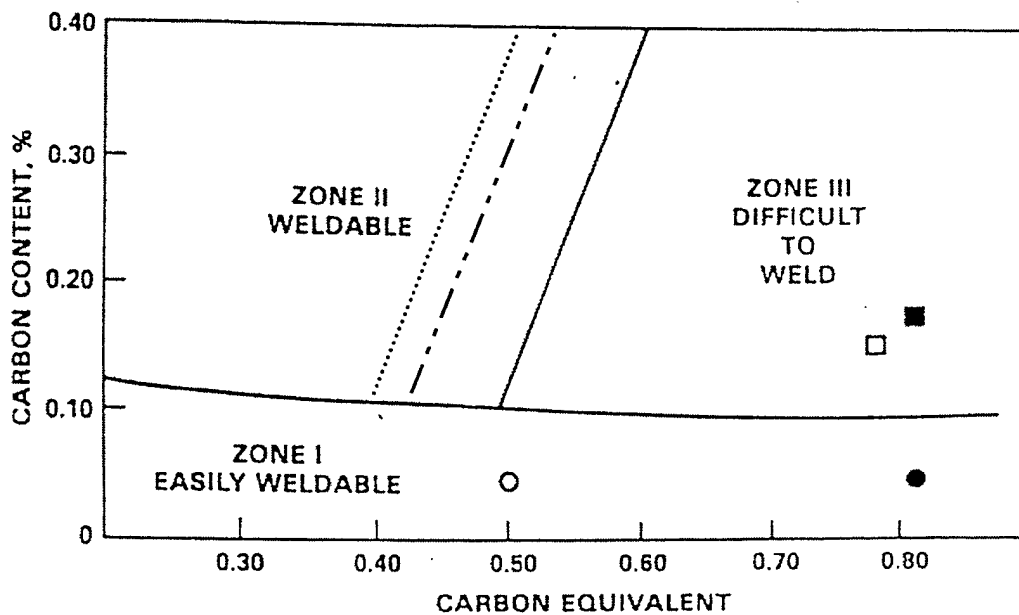
Figure 2.3 Weldability chart for various CE

D. SCOPE OF PRESENT WORK

Underwater wet welding using shielded metal arc welding (SMAW) on U.S.

Naval Vessels is very attractive because of the ability to effect repairs without costly dry

dock expenses. In the past the primary problems with underwater wet weldments on

steels utilizing SMAW with ferritic electrodes, were underbead cracking in the heat

affected zone (HAZ), slag inclusions, oxide inclusions, and porosity. This phenomenon

has been studied at Naval Post Graduate School on the weldablity of ASTM A6516

Grade 70 steel. Both LT Robert L. Johnson and LT Ryan D. Manning conducted the

thesis research. Their research considered the effects of water temperature and water

depth of steel weldments. The research found that underbead cracking occurred regardless

of water depth or temperature when wet welding ferritic steels with a mild steel ferritic electrode. Although, the cracking was less pronounced at higher water temperatures.

This research concentrates on three weld samples that were made using an austenitic nickel weld metal with an Oxylance coating at 10 feet of salt water, 25 feet of salt water, and 33 feet of salt water. A final sample was also made using austenitic nickel weld metal with a Broco coating at 33 feet of salt water. This approach was adopted to try and avoid underbead cracking.

This work addresses quality of the welds, mechanisms for the formation of the inclusions, and analysis of the difference between the Oxylance and Broco Ni-based weld rods.

THIS PAGE INTENTIONALLY LEFT BLANK

III. EXPERIMENTAL METHODS

The experimental procedures for the present work were derived from [Ref. 6] and [Ref. 7].

A. WELD SAMPLES

Four weld samples made on ASTM A36-96 steel were received from NAVSEA for analysis. All of the samples were welded using SMAW, welded in the overhead position. Three of the samples were welded utilizing a Sandvek electrode with a special coating at depths of 10, 25 and 33 feet of saltwater. This electrode consists of a 3/32-inch diameter nickel wire with a proprietary Oxylance waterproof coating. The samples are referred to as SNI-10, SNI-25, and SNI-33 respectively. The final sample was welded using a Sandvek electrode with a Broco underwater coating at the depth of 33 feet of saltwater; this sample is referred to as BNI-33. The Broco waterproof coating consists of aluminum and silicon in the form Al_3Si. All welds were performed on 5/8-inch thick plate of ASTM A36-96 steel with a B1V.1 joint restrained by 1/4-inch thick strong backs. The welding experiments were performed at Phoenix Marine in Berwick, LA. Welding parameters and conditions are listed in Table 3.1. The base metal for the four samples has a carbon equivalent of 0.36 wt% and 0.19 wt% carbon content.

Weld Sample	Welding Conditions and Parameters (Overhead Position)				
	Depth	Water Temp	# of Passes	Weld Rate	Weld Power
SNI-10	10 feet	49° F	23	5.53-7.50 in/min	2.1-3.3 kW
SNI-25	25 feet	49° F	25	5.50-8.33 in/min	2.4-3.0 kW
SNI-33	33 feet	75° F	29	6.49-8.57 in/min	2.8-3.5 kW
BNI-33	33 feet	75° F	35	6.96-11.16 in/min	2.5-3.0 kW

Table 3.1 Welding conditions and parameters

B. SAMPLE PREPARATION

The SNI-10, SNI-25, SNI-33 and BNI-33 welds were sectioned using a Powermet 2000 Automatic Abrasive Cutter from the 8-inch samples provided. There are eight total samples (2 SNI-10, 2 SNI-25, 2 SNI-33, and 2 BNI-33), with the following approximate dimensions: 2 3/4 x 5/8 x 7/8 inches. The eight samples were prepared for analysis by wet sanding using a Buehler Ecomet 4 utilizing 180, 320, 500, 1000, 2400, and 4000 grit Struers waterproof silicon carbide paper. The samples were then polished utilizing a Buehler microcloth and Buehler 3 μm diamond polish followed by 0.05 μm Buehler micropolish gamma alumina. Polishing was accomplished on the Buehler Ecomet 4.

The Oxylance and Broco electrodes were sectioned using the Buehler Isomet 2000 precision saw and then mounted using Buehler Probemet conductive molding compound in a Buehler Simplimet-2 mounting press. The mounted, sectioned electrodes were then prepared as the weld samples above.

The polished samples were examined in a scanning electron microscope (SEM). In order to conduct optical microscopy on the base metal, the polished samples were etched in 5% Nital solution for 5 seconds. Optical microscopy on the fusion zone was completed after the optical microscopy was completed on the base metal and the samples were etched in 5 grams Ferric Chloride and 50 ml HCl solution for 15 seconds. The samples were then stored in an evacuated chamber to slow corrosion.

C. SCANNING ELECTRON MICROSCOPY

The Topcon SM-510 scanning electron microscope was used to count and measure the inclusions present in each sample. This was accomplished by obtaining 50

12

inclusion fields in the fusion zone at 7000x magnification (1464.43 μm^2) of each of the eight samples. There are 25 fields from the two samples from each category. From the information obtained from the 50 inclusion fields of each sample, the average size, volume fraction, and standard deviation were found. An Oxford Link Gem Energy dispersive analysis of emitted x-rays (EDX) detector, utilizing Link ISIS software was used to identify the chemical make up of inclusions, fusion zone, both electrodes, and Ni segregation into the base metal. An EDX line scan was conducted on all four samples at the cap and root of the welds with magnification of 88x and 1000x at each location, to search for possible Ni segregation.

D. OPTICAL MICROSCOPY

After the samples were etched, optical microscopy was conducted using a Carl Zeiss Jenaphot 2000 optical microscope. A Pulnix TMC-74 camera with Semicaps software was used to obtain micrographs from the fusion zone, HAZ, and base metal. Macroscopic photographs were taken using a Sony Digital Maciva MVC-FD81 hand held digital camera.

E. MICROHARDNESS

A Buehler Micromet 2004 microhardness testing machine with a 200-gram load was used to conduct microhardness reading in Hardness Vickers (HV). Readings were obtained from both sides of the weld near the cap of the final weld pass from the base metal to the fusion zone, and a reading in the middle of the fusion zone.

THIS PAGE INTENTIONALLY LEFT BLANK

IV. RESULTS AND DISCUSSION

A. WELD METAL AND ELECTRODE COMPOSITION

The composition of the weld metal and the electrode filler rod and flux were found using SEM/EDX as described in section III.

1. Weld Metal Composition

The results of the weld metal compositions from the middle of the fusion zone are presented in Table 4.1. The composition of the weld metal is dependent on a variety of factors. These factors are base metal composition, filler rod composition, flux composition, effects of hyperbaric pressure, and dissociation of H_2O into hydrogen and oxygen [Ref. 8]. The results presented in Table 4.1 represent, fairly accurately, the overall composition of the weld metal. However, the data does not include light elements that appear in small amounts as it is difficult to quantify them by EDX. Consequently, oxygen and carbon contents were not determined for any of the samples although these will be small (<< 0.1 wt%). As seen for Table 4.1, all samples have very similar chemical compositions. The iron in the weld metal comes from dilution of the base plate as well as from the weld rod electrode covering. The chromium and sulfur in the weld metal both come from the electrode flux coating (see Table 4.2). The Ni-Fe-Cr phase diagram predicts austenitic alloys for these compositions and these of course will be stronger than pure nickel due to alloying. This alloying effect will hopefully produce a weld metal of sufficient strength for the base plate concerned.

Weld Metal Composition											
SNI 10			SNI 25			SNI 33			BNI 33		
	Weight %	Atomic %		Weight %	Atomic %		Weight %	Atomic %		Weight %	Atomic %
Si	0.33	0.66	Si	0.36	0.71	Si	0.29	0.58	Si	0.31	0.62
S	2.42	4.20	S	2.38	4.15	S	2.30	4.00	S	2.41	4.19
Cr	14.77	15.84	Cr	14.28	15.33	Cr	14.58	15.66	Cr	15.12	16.21
Mn	2.82	2.87	Mn	2.68	2.72	Mn	2.76	2.81	Mn	2.74	2.78
Fe	15.34	15.33	Fe	15.07	15.07	Fe	16.09	16.09	Fe	15.89	15.87
Ni	64.32	61.11	Ni	65.23	62.02	Ni	63.98	60.86	Ni	63.53	60.33

Table 4.1 Weld metal Composition

2. Electrode Composition

Both electrodes were sectioned, mounted, and then analyzed with the SEM/EDX. SEM images of the Sandvek electrodes with Oxylance and Broco coatings are presented in Figures 4.1 and 4.2 respectively. These images show the cross-section of the filler rod and flux. EDX analysis was conducted on the filler rod,. the flux and the special waterproof coating. EDX analysis gives the overall compositions of the electrodes, which are presented in Table 4.2. Figures 4.3 and 4.4 show the overall composition EDX spectra from the both Sandvek electrodes, with Oxylance and Broco coatings respectively. The flux of each electrode is made up of the some compounds that could be identified, however the other elements could not be detected in association with a compound, although it is very likely that CaO, K_2O, Al_2O_3, and SiO_2 are present in the flux. This sort of flux component is typical of those associated with basic electrodes. As discussed in Section II, both electrodes are coated with a waterproof coating to prevent water absorption during underwater operations. The Oxylance coating is a TiO_2 filled polymer coating. The Broco coating was found to be an aluminum-silicon alloy, which was discussed in [Ref. 6]. The waterproof coating serves to prevent water absorption and also

16

assist in deoxidizing the weld metal by forming oxide inclusions in the fusion zone [Ref. 9].

EDX results of Sandvek electrodes		
	Oxylance Coating	Broco Coating
Filler Metal	Ni	Ni
Flux	$FeCr,FeS_2,CaF_2,O,Al,Si,K$	$FeCr,FeS_2,CaF_2,O,Al,Si,K$
Coating	TiO_2 filled polymer	Al_3Si

Table 4.2 Electrode compositions
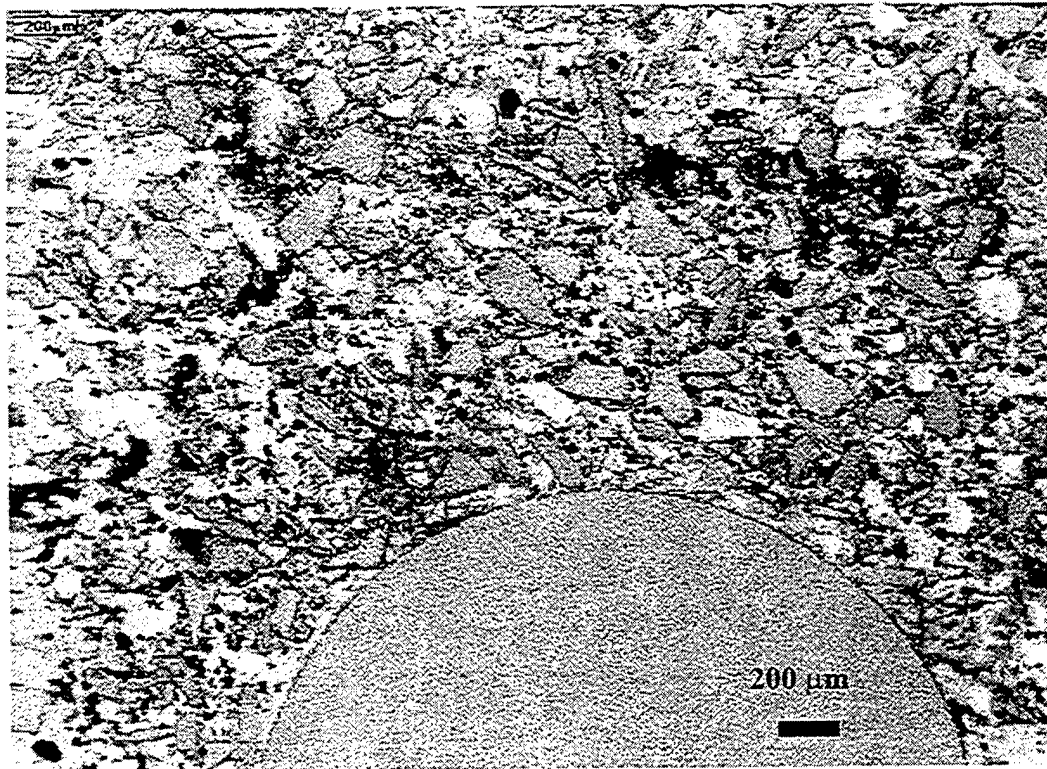
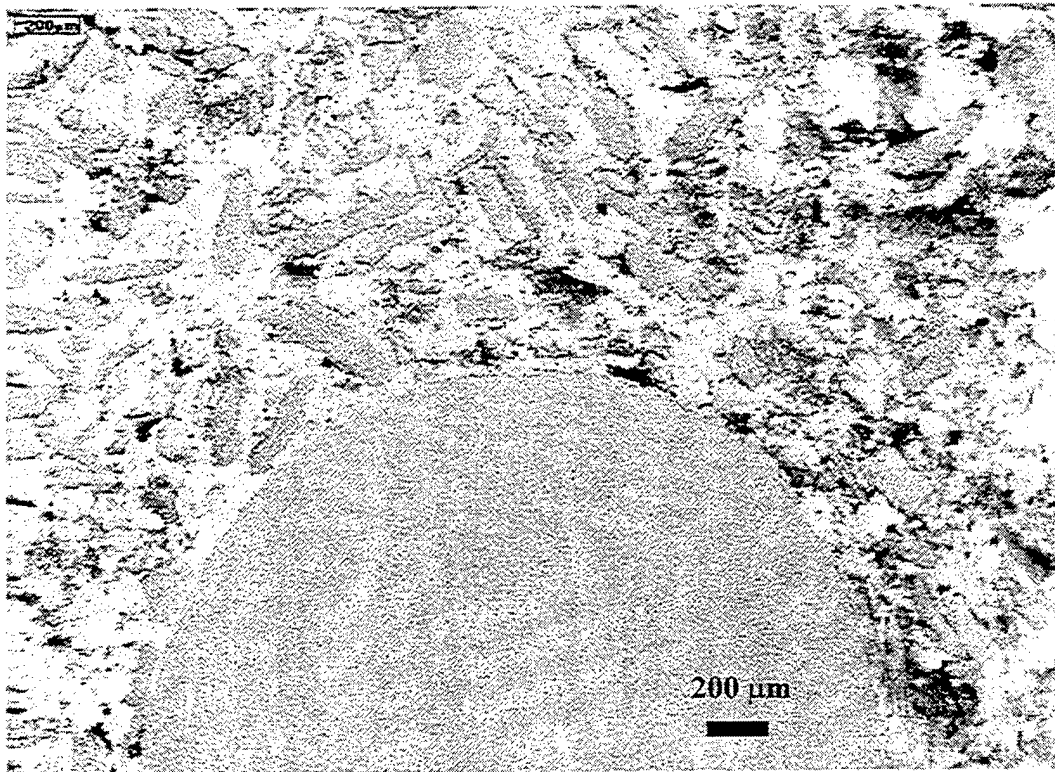Figure 4.1 Sandvek electrode cross-section with Oxylance coating
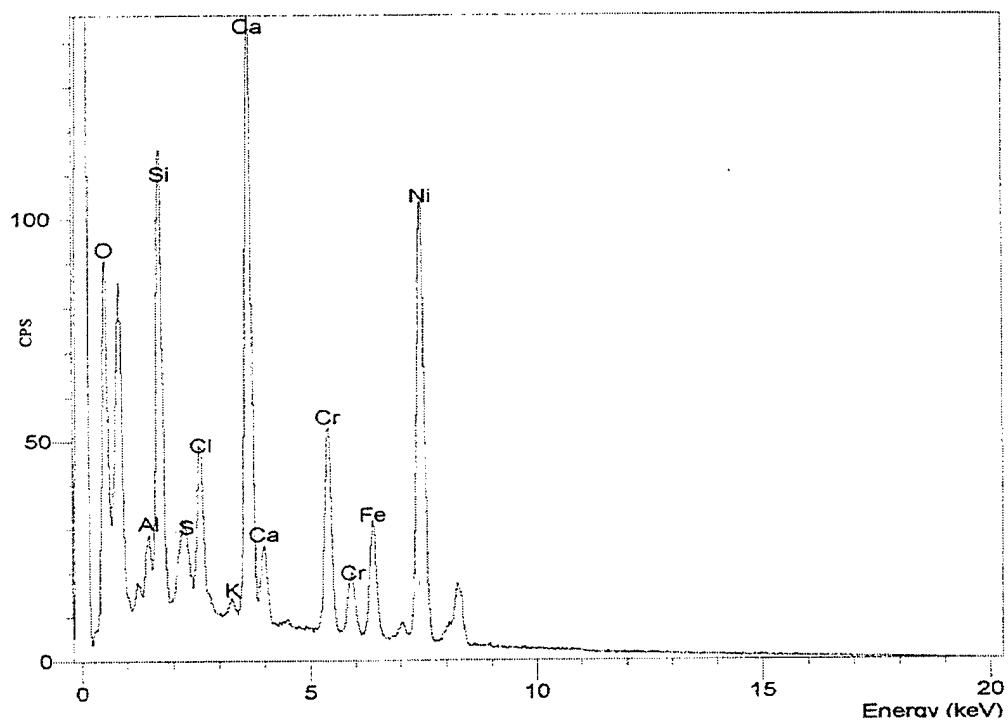
Figure 4.2 Sandvek electrode cross-section with Broco coating

Figure 4.3 EDX spectrum of Oxylance electrode
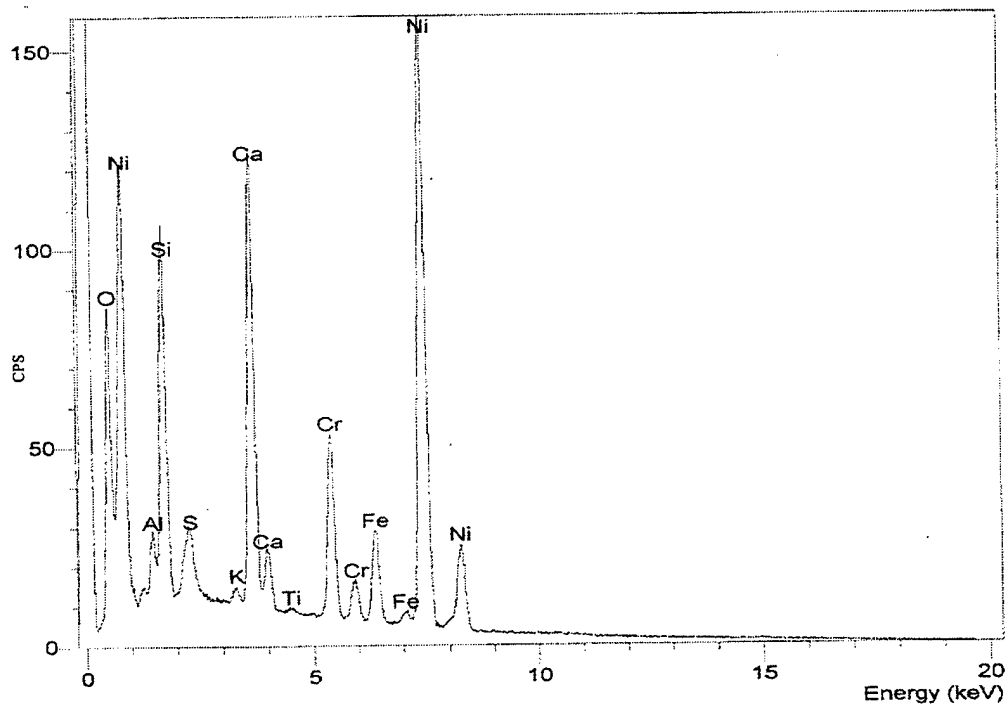
Figure 4.4 EDX spectrum of Broco electrode

B. NICKEL SEGREGATION IN THE BASE AND WELD METAL

EDX line scans were conducted on all four weld samples to determine any
possible Ni segregation into the base metal as described in section III. Figures 4.5 and 4.6
show SEM images of SNI-25 with typical line scan at the cap at 88x magnification and
the root at 1000x magnification of the weld respectively. The corresponding results from
the line scan in Figure 4.5 and 4.6 are shown in Figure 4.7 and 4.8. The line perpendicular
to the line scan shows where the fusion zone meets the HAZ. It can be seen in Figure 4.7
and 4.8 that there is very little Ni migration from the fusion zone into the base metal. The
Fe in the weld metal will consist of Fe from the electrode and from base metal dilution.
The weld metal appears to be homogenous (except for inclusions) and the spikes in the Al
and O scans just inside the base metal come from inclusions.
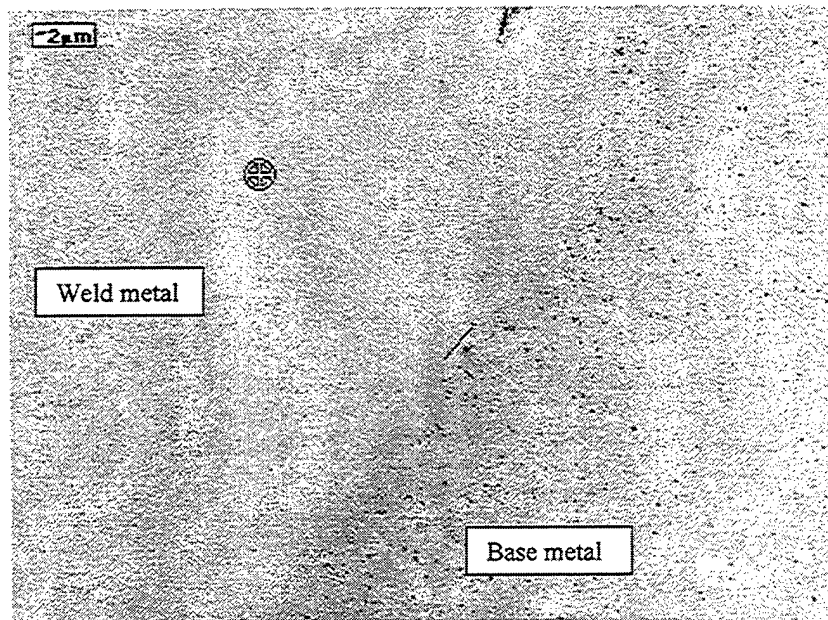
Figure 4.5 SEM image with line scan at 88x
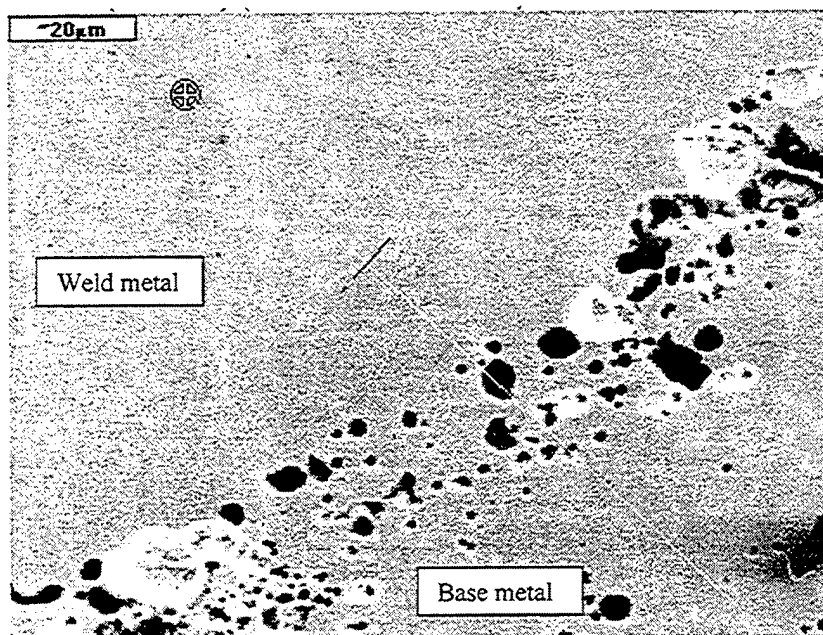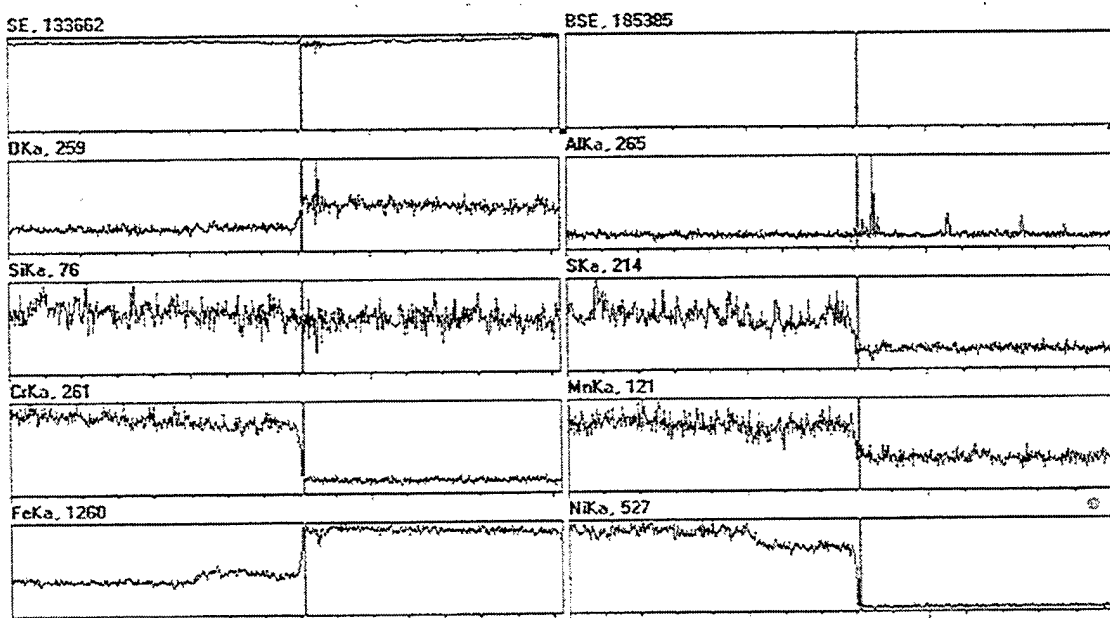
Figure 4.6 SEM image with line scan at 1000x

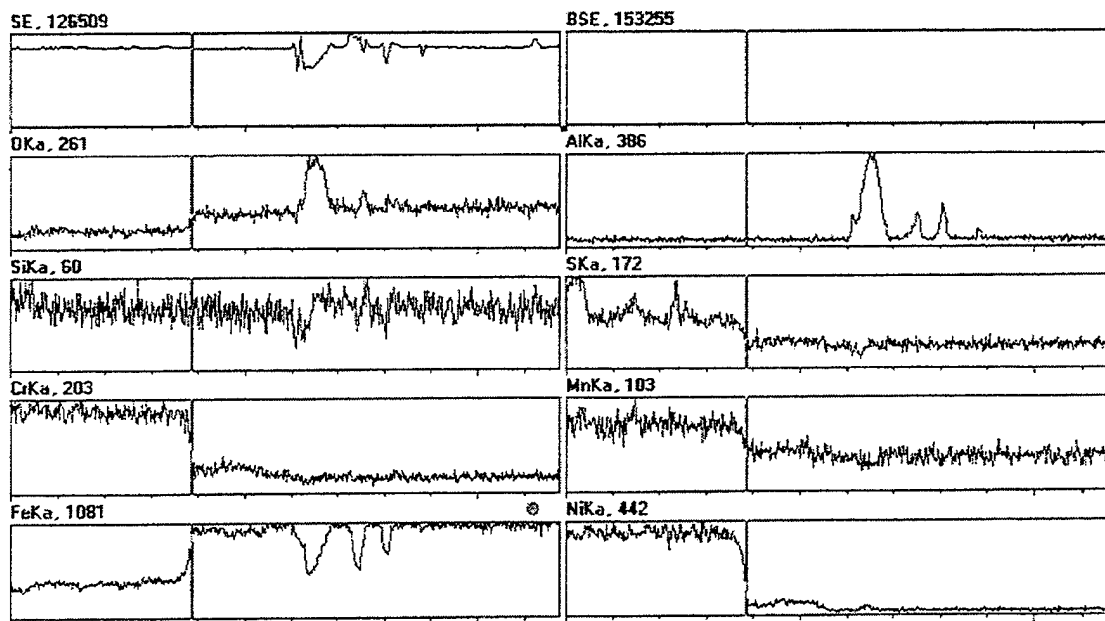Figure 4.7 EDX line scan results from the top of sample at 88x

21

Figure 4.8 EDX line scan results from the top of sample at 1000x

C.   NON-METALLIC INCLUSIONS

1.   Size and Volume Fraction

As in [Ref. 6] and [Ref. 7] an analysis of the inclusions in the fusion zone was conducted. The inclusions were counted and measured to find mean diameter, standard deviation, confidence and volume fraction. Figure 4.9 shows a typical inclusion field that was used to count and measure the inclusions. Table 4.3 shows the results from the analysis of the oxide inclusions. From Table 4.3 one can see that the average size of the inclusions increases as depth increases. However, the volume fraction at SNI-10 and SNI-25 are approximately the same, but SNI-33 has an increased in volume fraction of oxide inclusions. BNI-33 on the other hand has a much smaller inclusion volume fraction. From gamma ray non-destructive testing (NDT) it was found that the BNI-33 had much great

22

porosity than the other three samples. SNI-33 and BNI-33 have very different welding procedures, different weld speeds and number of passes. Also, the electrodes have different waterproof coatings. It was concluded that the increase in porosity, which is detrimental to the weld strength, is due either to the difference between the coatings of the two electrodes and/or the higher number of passes required to complete the BNI-33 weld. Although many more weldments need to be studied to be completely confident of this assertion.
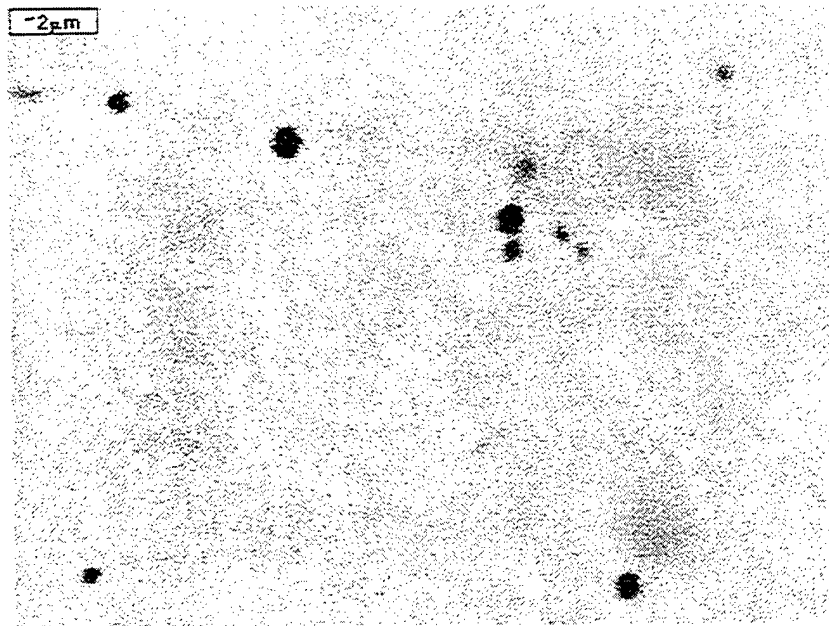
Figure 4.9 Typical inclusion field

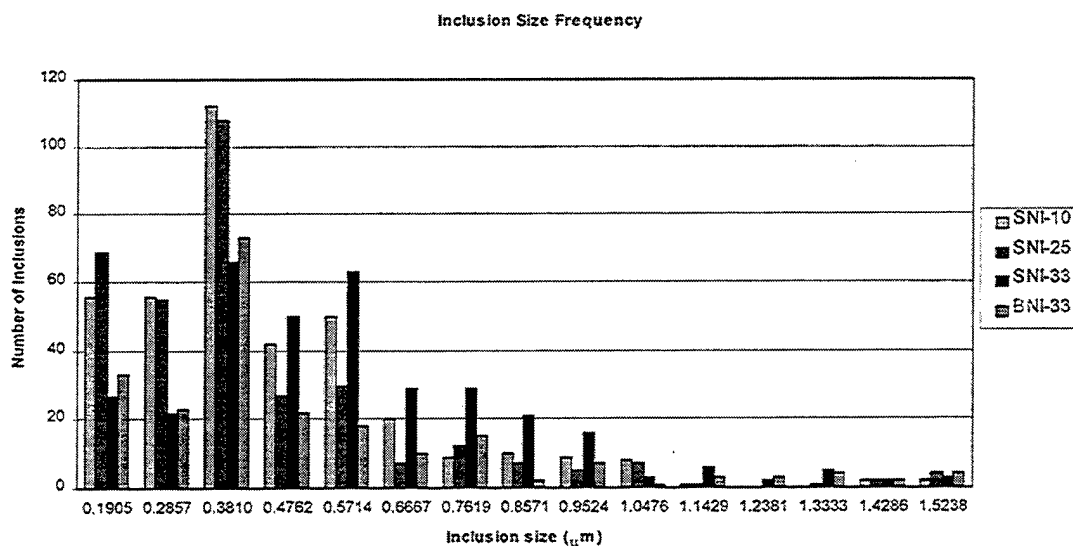| Inclusion Data				
	SNI 10	SNI 25	SNI 33	BNI 33
Average Size	0.4629	0.4725	0.5851	0.5660
Standard Deviation	0.2561	0.5186	0.3074	0.4743
Confidence	0.033881	0.072531	0.042491	0.081064
Volume Fraction	0.000871	0.000812	0.001274	0.00078

Table 4.3 Inclusion Data

Figure 4.10 Histogram of inclusion size

2.   Inclusion Microchemical Analysis

Oxide inclusions are formed in the fusion zone during solidification. These

inclusions were studied using EDX to determine chemical composition. The resulting

inclusions were found to have MnO, MnS, SiO_2, Al_2O_3, TiO_2, and CaO present and have

close to a spherical morphology. Figure 4.11 and 4.12 shows a typical oxide microprobe

location and an inclusion EDX spectrum respectively. The remaining elements present in

the EDX spectrum are attributed to the weld metal matrix, although some Cr_2O_3 may be

present in the inclusions. The microprobe position in Figure 4.11 is shown by the circle

with a '+' in the middle.

It was difficult to examine smaller inclusions because they would return a similar

EDX spectrum to the weld metal. This is due to the bulb of interaction of the microprobe.

This bulb of interaction is shown in Figure 4.12 [Ref. 10] Due to the small diameter of

the inclusions, the bulb interacts predominantly with the weld metal underneath the

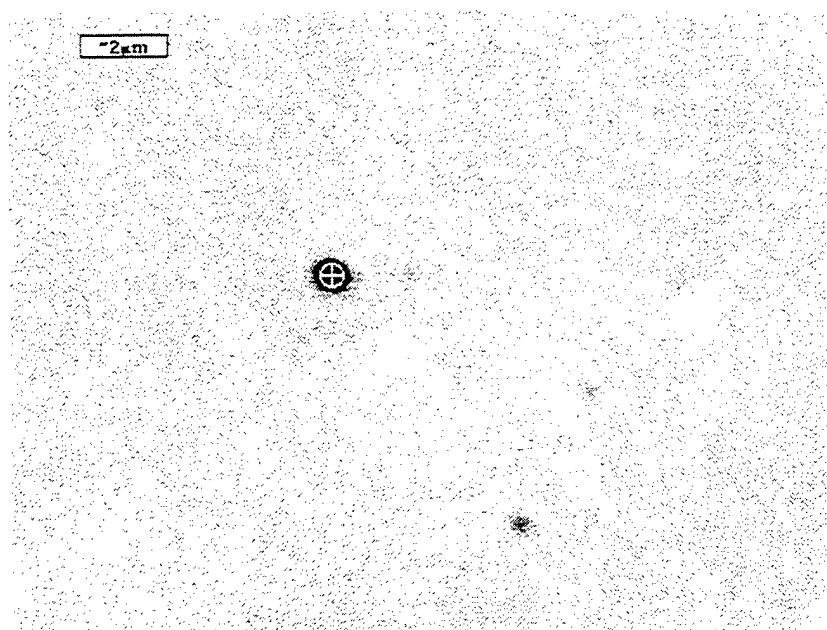inclusion resulting an EDX spectrum that is very similar to the weld metal.
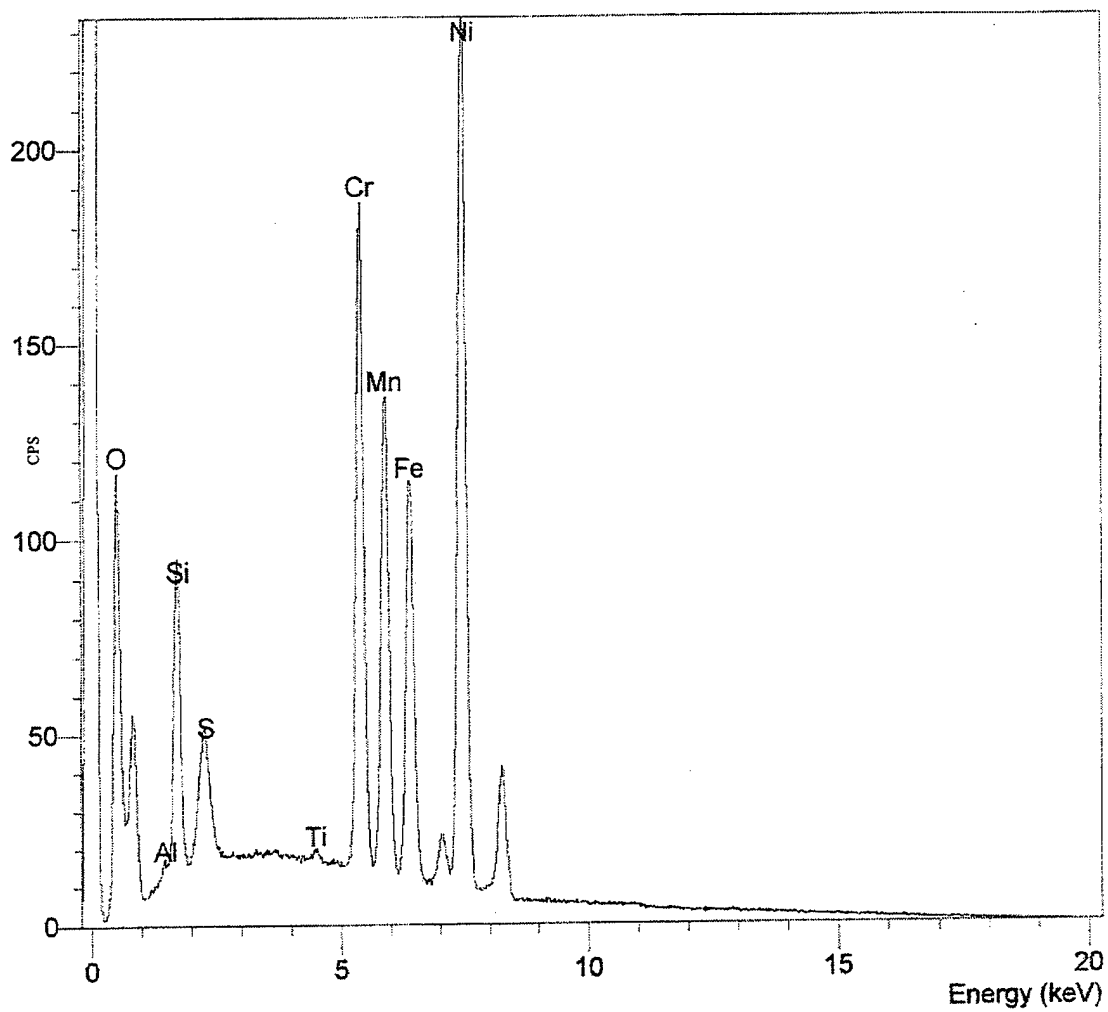

Figure 4.11 EDX microprobe on inclusion
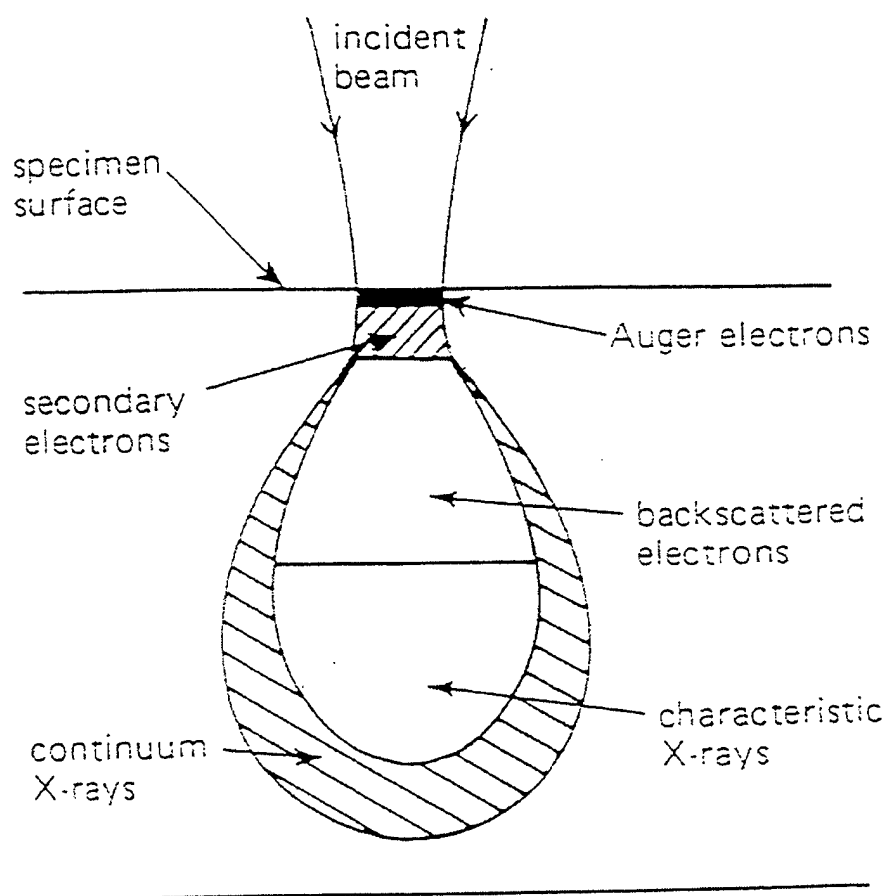
Figure 4.11 EDX spectrum of typical oxide inclusion

Figure 4.12 Generation of electrons and x-rays in a sample [Ref. 10]

D.   MICROHARDNESS ANAYLSIS

Hardness tests were conducted on all four samples in accordance with section III.

Figure 4.13 shows the location of the hardness tests. The results of the hardness test are

tabulated in Table 4.4. The hardness results were consistent throughout all four samples,

which can be seen in Figure 4.14 and the weld metals are clearly at least as strong as the

base plate. These electrodes could thus perhaps be used for underwater wet welding of

slightly stronger (higher CE) steels than the one studied in the present work.
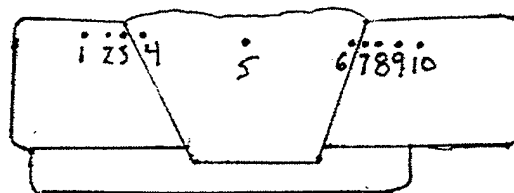
Figure 4.13 Hardness testing positions

Hardness Results (Vickers Harness)				
		SNI 10	SNI 25	SNI 33	BNI 33
1	Base metal	201.9	222.2	186.4	213.2
2	HAZ	252.1	264.4	251.5	270.9
3	HAZ	256.8	233.5	258.1	297.6
4	Fusion zone	259.5	253.4	247.6	235.3
5	Middle of Fusion zone	279.1	261.6	268.0	258.8
6	Fusion zone	256.1	230.6	229.4	249.5
7	HAZ	270.9	260.2	252.8	315.2
8	HAZ	243.2	222.7	223.8	271.6
9	Base metal	205.8	187.7	218.4	229.4
10	Base metal	200.5	213.2	192.0	207.7

Table 4.4 Hardness results

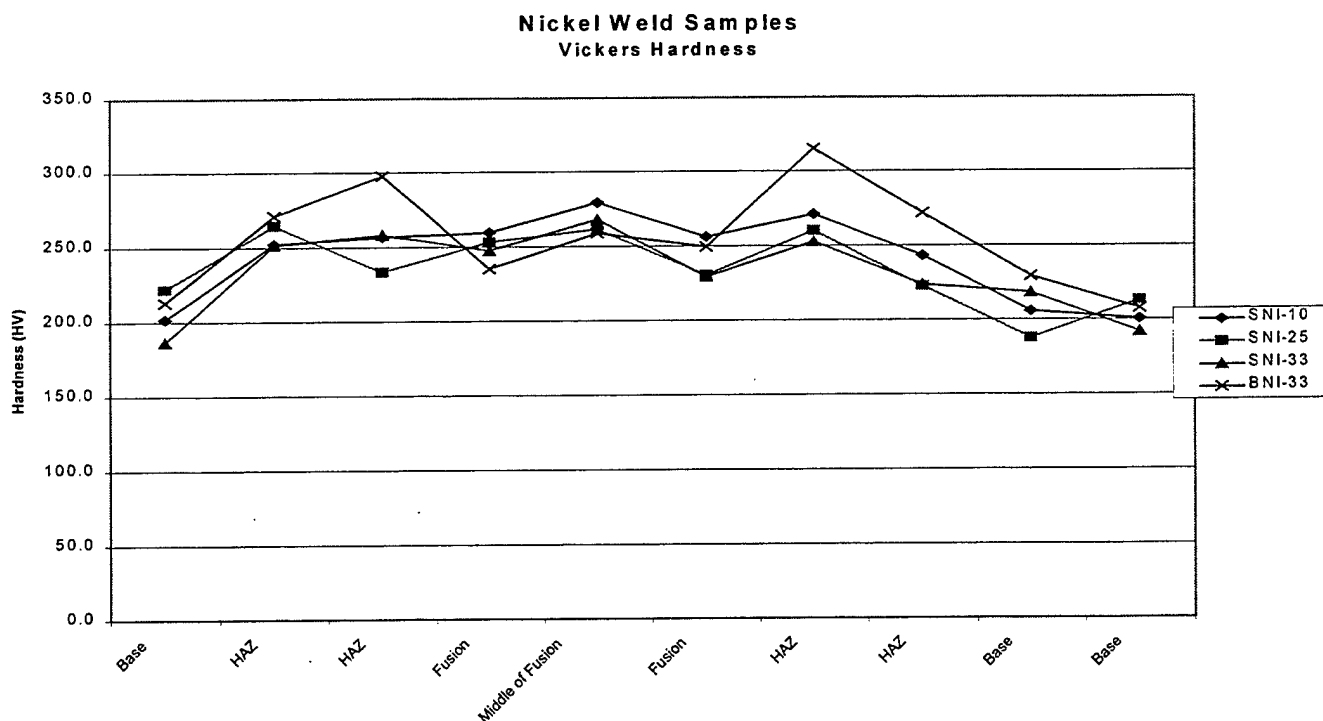**Nickel Weld Samples**
Vickers Hardness

Figure 4.14 Plot of hardness results

E. MICROSTRUCTURAL ANALYSIS

1. Macroscopic

The macroscopic micrographs are represented in Figures 4.15 through 4.18 and

are of SNI-10, SNI-25, SNI-33, and BNI-33 respectively. All four samples were etched in

a 5% Nital solution for 5 seconds prior to the photographs. From the images it can be

seen that there is porosity present in three out four weld samples but underbead cracking

could not be found at any magnification. Only one cross-section from each was studied

and so the extent of the porosity could not be assessed by optical microscopy alone.

However, as mentioned previously, gamma radiography performed on all four samples

indicated that the weld metal obtained using the electrode with the Broco (Al_3Si) coating

showed much more porosity than the other samples (Sandvek with the polymer/TiO_2 coating).
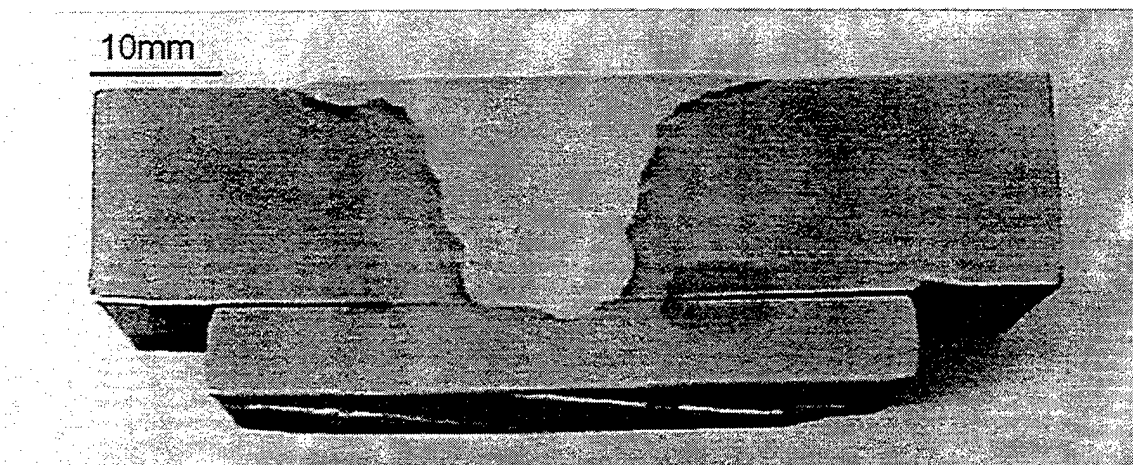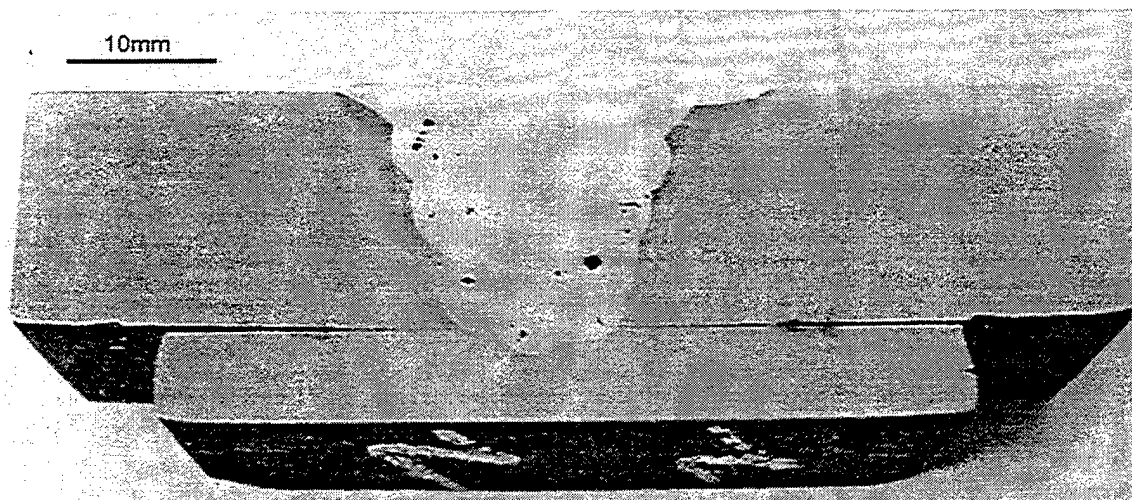

Figure 4.15 Macroscopic image of SNI-10

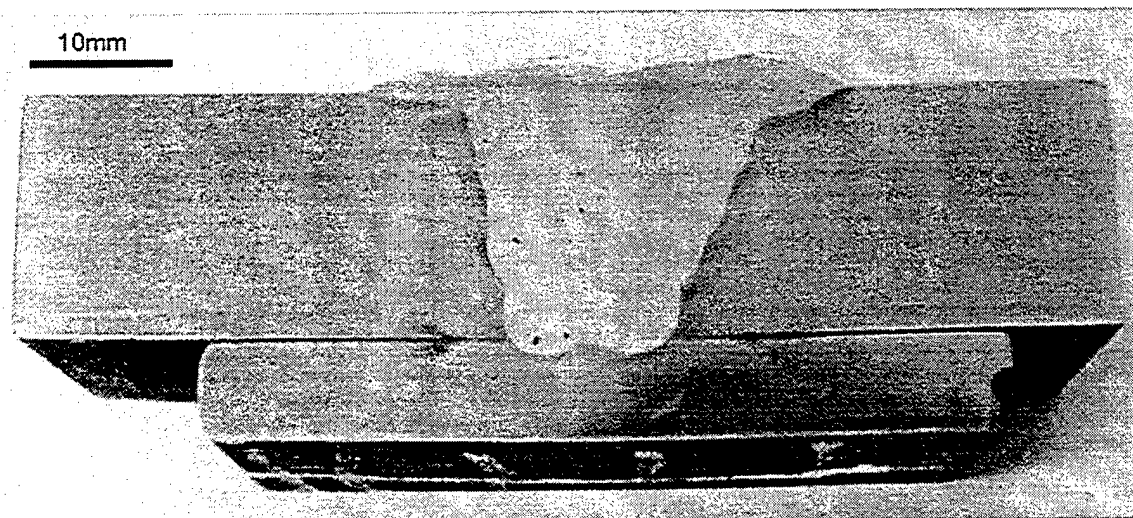Figure 4.16 Macroscopic image of SNI-25
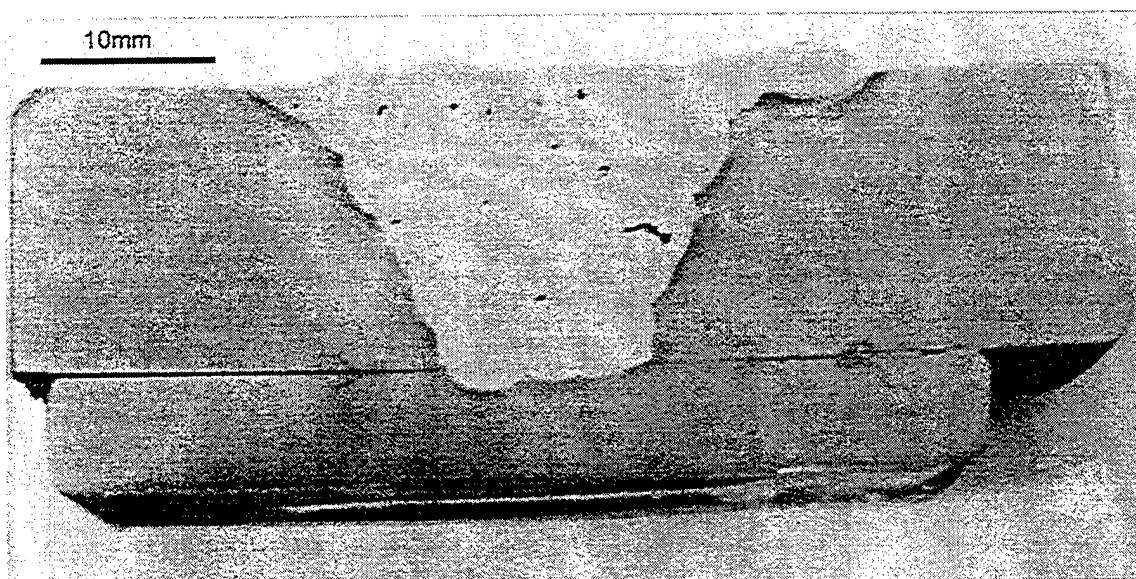
Figure 4.17 Macroscopic image of SNI-33

Figure 4.18 Macroscopic image of BNI-33

2. Microscopic

All four samples were etched as explained in section III and then examined in the optical microscope. The microstructure of the HAZ is very similar to the findings in [Ref. 6] and [Ref. 7]. The HAZ was found to consist mostly of Widmanstatten ferrite, grain boundary ferrite, martensite and banite. The microstructure of the HAZ through the base

31

metal can be seen in Figure 4.19 through Figure 4.23. The microstructure of Fusion zone was found to consist of columnar grains of a single-phase alloy as discussed in [Ref. 4]. The Fusion zone microstructure is represented in Figure 4.12.
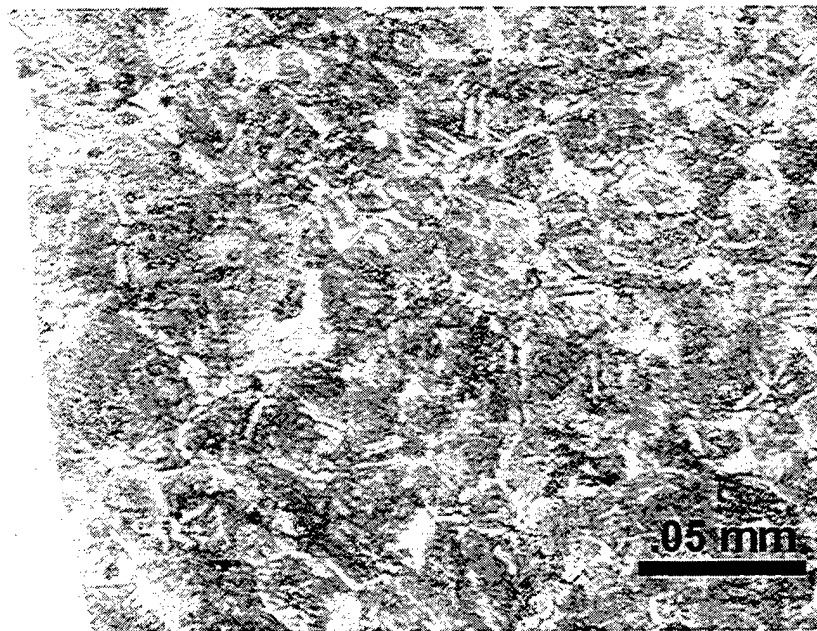

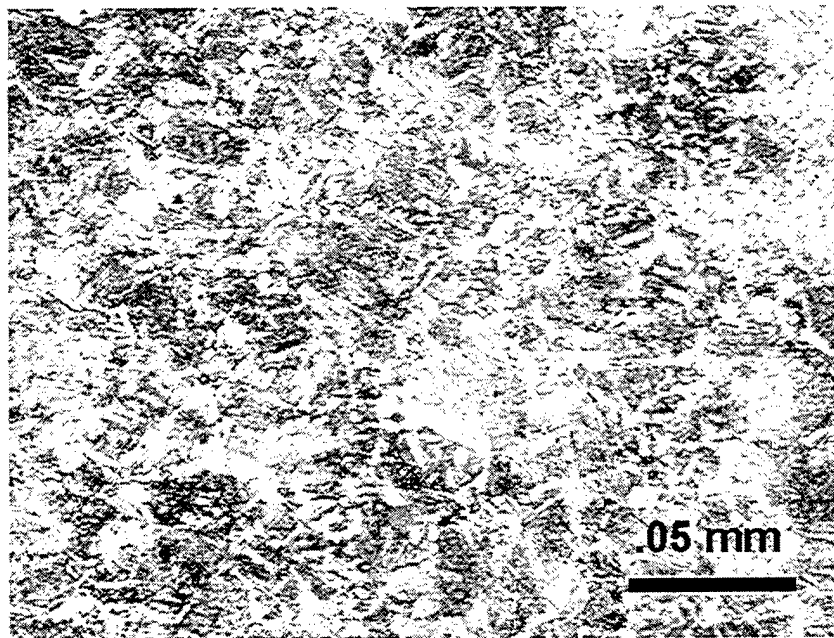Figure 4.19 Micrograph of SNI-33 at the edge of the fusion zone in the HAZ

Figure 4.20 Micrograph of SNI-33 in the HAZ

Figure 4.21 Micrograph of SNI-33 in the grain refinement region of the HAZ
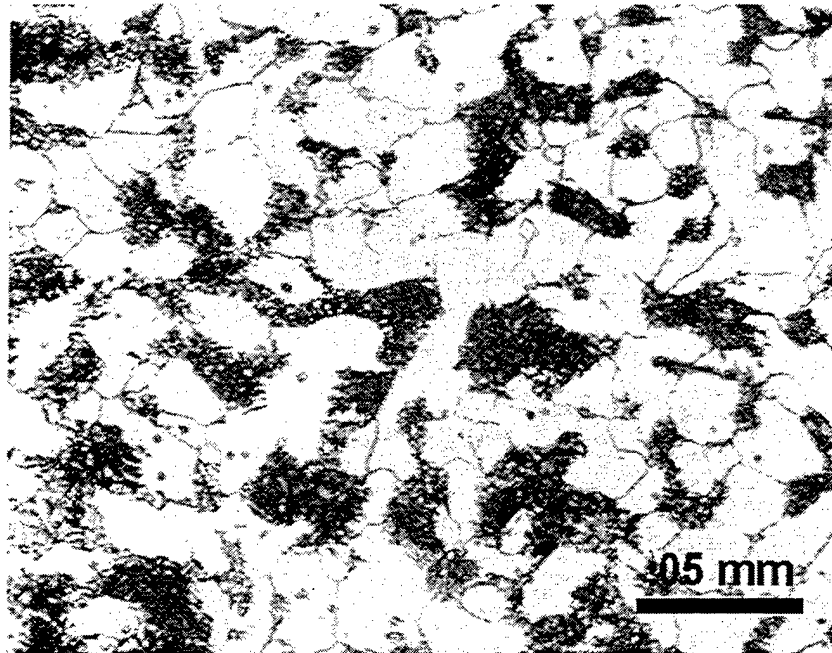
33

Figure 4.22 Micrograph of SNI-33 in the coarse grain region of the HAZ
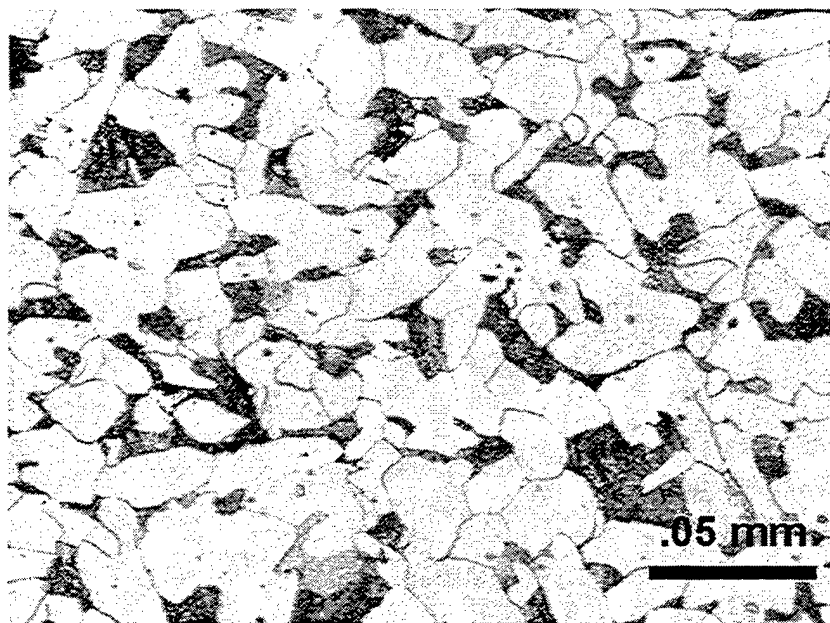

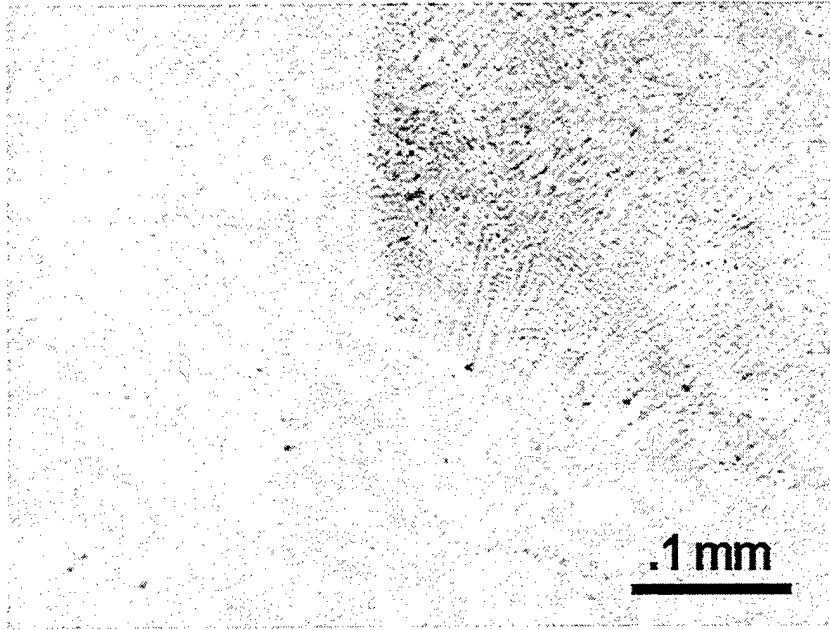Figure 4.23 Micrograph of SNI-33 Base metal
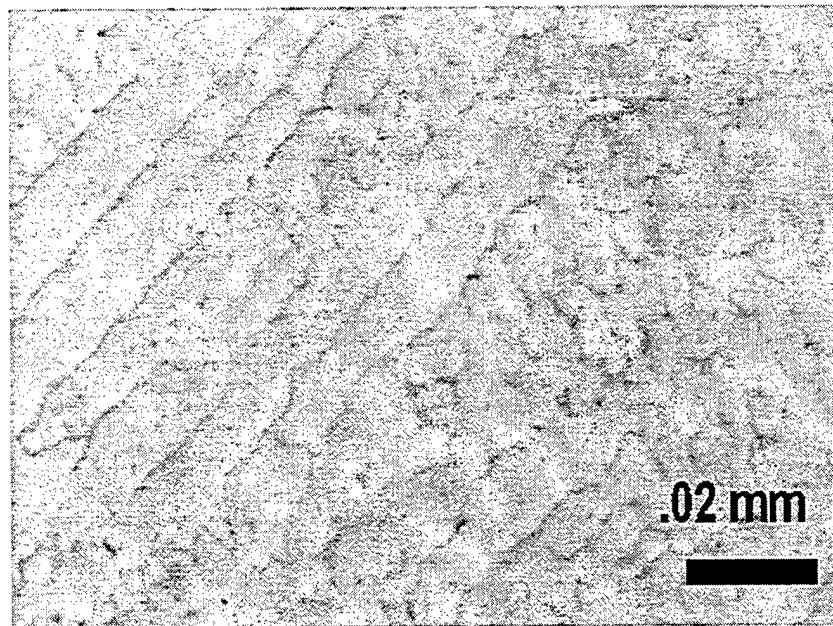
Figure 4.24 Micrograph of BNI-33 fusion zone

Figure 4.25 Micrograph of BNI-33 fusion zone columnar grains

THIS PAGE INTENTIONALLY LEFT BLANK

V. CONCLUSIONS AND RECOMMENDATIONS

A. CONCLUSIONS

In previous research [Ref. 6] and [Ref. 7] the amount of underbead cracking found in the underwater welds was very significant when ferritic electrodes were used. However, with the use of a nickel based alloy in the fusion zone the problem was eliminated, despite the presence of martensite in the HAZ. Nickel segregation within the weld metal was found to be negligible at the cap and the root of all four weld samples. The inclusion information that was gathered from the weld metals associated with the Oxylance samples suggests that there is an increase in oxide inclusions volume fraction with increasing water depth. The weld metal of the Broco sample had a somewhat lower inclusion volume fraction but suffered from severe porosity. The strength of all four samples were very similar and the weld metal strength closely matched that of the base metal indicating that nickel alloys can be effective weld metals from a strength point of view.

B. RECOMMENDATIONS

In this research the quality of underwater wet welds produced using austenitic Ni-based electrodes was examined and found to be adequate for ASTM A36-96 steel with the Oxylance electrode. For further research, it is recommended to study the inclusion fields in the Oxylance samples to discover the process and mechanisms for the formation of the inclusions and porosity detrimental to mechanical properties. The use of electrodes with the Broco (Al_3Si) coating should be discontinued unless further work indicates that the porosity detected in the present work is a 'one off' due to excessive numbers of weld

passes or that the porosity can be eliminated in some way.

LIST OF REFERENCES

1. AWS Committee on Welding in Marine Construction, "Specification for Underwater Welding", *American Welding Society*, (ANSI/AWS D3.6-93), August 1992.

2. Silva, E.A., "Underwater Welding and Cutting", Metals Handbook, 9th Edition, vol. 6, American Society of Metals, 1983.

3. Naval Sea Systems Command, *U.S. Navy Underwater Cutting and Welding Manual,* 1 April 1989.

4. Kou, S., *Welding Metallurgy,* John Wiley and Sons, 1987.

5. Dill, J.F., "Model For Estimation of Thermal History Produced by a Single Pass Underwater Wet Weld", Thesis, Naval Postgraduate School, December 1997.

6. Johnson, R.L., "The Effect of Water Temperature on Underbead Cracking of Underwater Wet Elements", Thesis, Naval Postgraduate School, September 1997.

7. Manning, R.D., 'Analysis of Underbead Cracking in Underwater Wet Weldments on A516 Grade 70 Steel", Naval Postgraduate School, September 1998.

8. Ibarra, S.S. Liu and D.L. Olson, "Underwater Wet Welding of Steels", *Welding Research Council Bulletin,* no. 401, pp. 1-39, May 1995.

9. Sanchez-Osio, A. and S. Liu, "Influence of Consumable Composition and Solidification on Inclusion Formulation and Growth in Low Carbon Steel Underwater Welds", *Welding Research Council Bulletin*, no. 399, pp. 1-59, February 1995.

10. Smallman, R.E., *Modern Physical Metallurgy,* Butterworth-Heinemann Ltd. 1992.

THIS PAGE INTENTIONALLY LEFT BLANK

INITIAL DISTRIBUTION LIST

1. Defense Technical Information Center................................... 2
    8725 John J. Kingman Rd., Ste 0944
    Ft. Belvoir, VA 22060-6218

2. Dudley Knox Library.. 2
    Naval Postgraduate School
    411 Dyer Rd.
    Monterey, CA 93943-5101

3. Naval/Mechanical Engineering Curricular Office, Code 34............ 1
    Naval Postgraduate School
    Monterey, CA 93943-5100

4. Department Chairman, Code ME....................................... 1
    Department of Mechanical Engineering
    Naval Postgraduate School
    Monterey, CA 93943-5101

5. Dr. Alan G. Fox.. 2
    Department of Mechanical Engineering
    Naval Postgraduate School
    Monterey, CA 93943-5101

5. Mr. Michael Dean, SEA OOC5.. 2
    Supervisor of Salvage and Diving
    Naval Sea Systems Command
    Arlington, VA 22242-5160

6. LT Brian J. Sheakley.. 2
    5550 S.E. Sun Meadow Terrace
    Milwuakie, Or, 97267